Nanostructures

Deutsche Ausgabe: DOI: 10.1002/ange.201603456
Internationale Ausgabe: DOI: 10.1002/anie.201603456

Controlled Growth of a Hierarchical Nickel Carbide "Dandelion" Nanostructure

*Liang Qiao, Wenxia Zhao, Yueling Qin, and Mark T. Swihart**

Abstract: *We present a new type of highly hierarchical but nonporous nanostructure with a unique "dandelion" morphology. Based on the time evolution of these Ni_3C nanostructures, we suggest a mechanism for their formation. This type of hierarchical nanocrystal, with high accessible specific surface area in a relatively large (ca. 750 nm overall diameter) stable structure, can be valuable in catalysis and related applications.*

Transition-metal carbides (TMCs), for example, Ni_3C, Mo_2C, and WC, can exhibit high electrical and thermal conductivity combined with excellent thermal and mechanical stability owing to their mixed covalent–ionic bonding.[1] TMCs can be excellent catalysts with performance comparable to noble metals for some reactions, and can also serve as supports for noble metal catalysts.[2] Recent studies have demonstrated TMCs' potential for application in electrical energy storage,[3] oxygen reduction,[4] hydrogen evolution,[5] and carbon nanotube fabrication.[6] Rhombohedral nickel carbide, Ni_3C, is a common product of nickel carburization during catalysis using Ni.[7] Nickel itself is a valuable catalyst from both industrial and academic perspectives.[8] Research on the transformation of Ni to Ni_3C helps elucidate its formation mechanism.

Solution-phase synthesis encompasses methods of preparing nanostructures as colloidal dispersions, often with precise control of their size and shape.[9] Controlled colloidal growth of nanocrystals (NCs) contributes to fundamental crystallization research by revealing interactions between crystal structure and the growth of specific ligand-passivated crystal facets. Development of novel nanostructures allows optimization of known properties and, in some cases, development of entirely new properties or behaviors. For a given amount of material, a hierarchical structure has larger surface area than a dense structure. More importantly, a hierarchical structure of the solid provides a hierarchical structure of the void spaces within it, which can make the surface area much more accessible than in a simple porous structure. Accessible surface area, along with intrinsic catalytic activity, determines the performance of catalysts. These factors have attracted many researchers' attention to hierarchical nanostructures.[10]

Few results of solution phase synthesis of Ni_3C have been reported. Goto et al. prepared Ni_3C dots by thermolysis of nickel acetylacetonate in oleylamine.[11] Sarac et al. investigated the branching of Ni_3C_{1-x} NCs.[12] Herein we report the synthesis of a hierarchical nonporous Ni_3C structure with high specific surface area by thermal decomposition of an organometallic Ni precursor in a mixture of ligands in a noncoordinating solvent.

As shown in Figure 1e, a typical hierarchical nanocrystal (HNC) consists of one core and many radially arranged branches, most of which are topped by a hexagonal cap. The HNCs can be figuratively referred to as "dandelion" flowers. Figure 1a, shows a bright–field (BF) TEM image of a hexagonal platelet capping one of the branches. The diffraction spots in the corresponding selected area electron diffraction (SAED) pattern, shown in Figure 1b, can be indexed to (006) planes of rhombohedral Ni_3C. Similarly, the SAED pattern in Figure 1d corresponds to the silhouette of a platelet and the supporting arm shown in Figure 1c. SAED patterns in Figure 1b,d jointly confirm that the platelets have large (001) hexagonal facets. Figure 1h shows the SAED pattern of several quasi-parallel branches, indicated by the blue square. Panel (f, g, and i) show dark field (DF) images corresponding to the $(\bar{1}1\bar{3})$, (006), and (113) diffraction spots, respectively. Figure 1f,i show clear stacking faults repeating along the axial direction, while absence of stacking faults in the (006) DF image (Figure 1g) implies that the displacement causing stacking faults is in the (001) plane, which is common for materials of the hexagonal crystal family including rhombohedral Ni_3C.

To understand the formation of the Ni_3C HNCs, we conducted time-resolved experiments (Figure 2). Quasi-spherical aggregates of primary particles, referred to as "cores", were observed after 75 min. In Figure 2g,m, the NCs on the aggregates' surface do not yet have well-defined shapes, but have begun to show a tendency to branch. The cross-section of the cores, Figure 2j, shows pores near the center, where primary particles may not yet have grown together, and pores near the surface, with a dense region between these porous zones. The atomic composition of these cores, obtained by energy-dispersive X-ray spectroscopy (EDS) is 84% Ni and 16% C. The Ni content at this point exceeds that of stoichiometric Ni_3C. After 80 min, the NCs have begun to branch, that is, the radial arms have grown in one dimension, and the platelets have begun to grow in the

[*] L. Qiao, Dr. W. Zhao, Prof. M. T. Swihart
Department of Chemical and Biological Engineering
University at Buffalo (SUNY)
Buffalo, NY 14260 (USA)
E-mail: swihart@buffalo.edu
Dr. W. Zhao
School of Chemistry and Chemical Engineering
Ningxia Normal University
Guyuan 756000 (China)
Dr. Y. Qin
Department of Physics, University at Buffalo (SUNY)
Buffalo, NY 14260 (USA)
Supporting information and the ORCID identification number(s) for the author(s) of this article can be found under http://dx.doi.org/10.1002/anie.201603456.

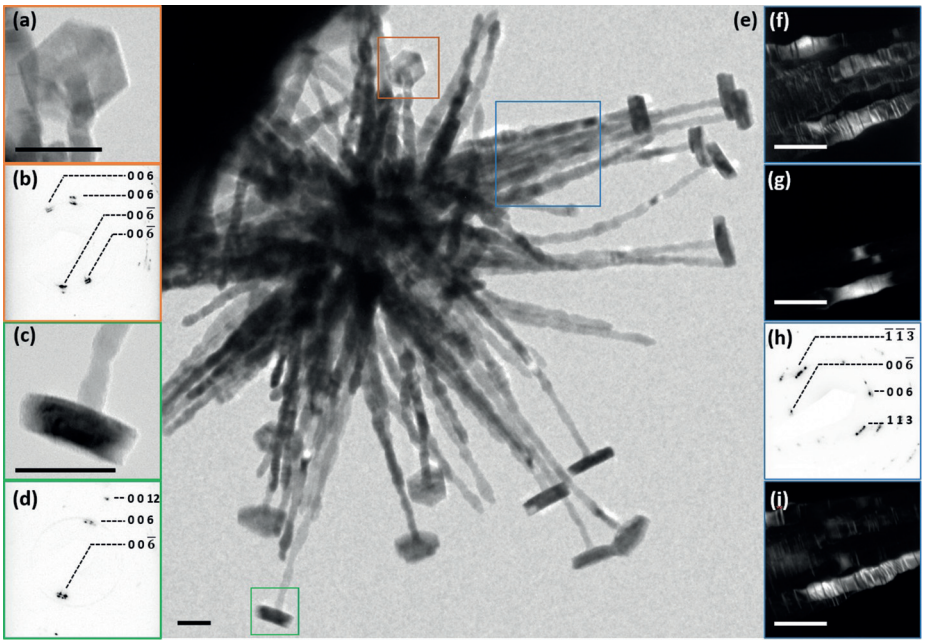

Figure 1. TEM images of one hierarchical nanocrystal (HNC). a,b) BF close-up and SAED pattern of a hexagonal platelet and attached arm, c),d) BF close-up and SAED pattern of the silhouette of a platelet, e) BF image of the whole hierarchical structure, f)–i) SAED pattern (h) and three related DF images (f),(g),(i) of several quasi-parallel branches. Colored squares indicate the studied areas. Scale bars: 50 nm.

perpendicular direction. From the 75th min to the 80th min, the cores blossomed into midsize HNCs, while also densifying to become non-porous, (Figure 2k). The composition of these HNCs, 50% Ni and 50% C, suggests that amorphous carbon may be trapped between the branches or coating parts of the structure.

Further growth of both the arms and the platelets proceeds through the 90th min. Figure 2f,i,o show images of the final "dandelions", whose average diameter is around 750 nm. The core remains solid, (Figure 2l). Additional cross-sections of the fully developed HNCs are provided in animation SM1 in the Supporting Information. The atomic composition of the HNCs matched the stoichiometry of Ni_3C, that is, 75% Ni and 25% C. During evolution from cores to dandelions, the specific surface area (SSA) increased from about 3 $m^2 g^{-1}$ to over 60 $m^2 g^{-1}$.

Cores and dandelions were further characterized by X-ray diffraction (XRD; Figure 3). Nickel has two common phases, hexagonal close-packed (HCP, Garutiite, $P6_3/mmc$) and face-centered cubic (FCC, $Fm\bar{3}m$). In the bulk, HCP is metastable, and FCC is the stable phase.[13] The XRD pattern of the cores matches that of HCP Ni, which suggests that the 16% carbon observed by EDS may be amorphous or adsorbed on the surface of the NCs. The fully developed HNCs have an XRD pattern consistent with rhombohedral Ni_3C[14] $(R\bar{3}C)$. Note that, owing to the similarity of their XRD patterns, Ni_3C has sometimes been mistaken for HCP Ni.[15]

The above results provide a basis for rational speculation on the HNCs' formation mechanism, as illustrated in Figure 4. Upon heating, the precursor, $Ni(acac)_2$, is converted to active monomers, probably nickel oleate.[16] The monomers accumulate to a supersaturation that triggers a burst of nucleation.[17] Moderate diffusional growth enlarges the nuclei to primary particles. The high concentration of primary particles leads to irreversible aggregation into cores.[18] Further growth by aggregation produces quasi-spherical structures of densely aggregated primary particles. The subsequent growth must be analyzed from several perspectives, because different parts of a HNC, that is, the core, the arms, and the caps, follow distinct growth mechanisms.

The cores must be porous upon formation by aggregation of primary particles. Annealing of the porous cores allows their reconstruction into a denser configuration. Simultaneous carburization can also expand the primary particles to fill voids in the aggregates. Each arm's axial elongation can occur by 1D growth from the cores (lower right corner of Figure 4). Initially, carbon accumulates in the cores, increasing from 16% to 50%, and the cores branch. When the branching is complete, the carbon content returns to 25%. It can reasonably be postulated that carbon may accumulate in the cores in an amorphous state, then combine with incoming Ni monomer or Ni from the core to form Ni_3C and elongate the arm in the axial direction. Possible mechanisms for the 1D growth include screw dislocation-driven growth, oriented attachment, or simple homogeneous epitaxy. The DF images, Figure 1f,g i, demonstrate stacking faults along the arms, and rule out the existence of screw dislocations. No rugged side faces can be observed in fully developed arms, Figure 1e, and the growth is continuous with the caps remaining at the end of the arms, so oriented attachment can be ruled out as well. Consequently, directional epitaxy is the most probable mechanism in this case. The most common phases of Ni, HCP and FCC, share intrinsic similarity. Thus, stacking faults can naturally arise during their layer-by-layer epitaxy. Comparing the HNCs at different times, it appears that the cores are partially consumed by growth of the arms. In addition to adsorbed ligands, the sidewalls of the growing arms may be coated by a layer of amorphous carbon that helps guide anisotropic growth. The presence of the caps at the end of the arms suggests that growth may be occurring at the base of the arms. The 2D growth of the platelets may follow the wedding cake growth mechanism[19] (Figure S4). Based on Figure 2g and Figure 2m, the NCs at the surface of the cores do not have defined shapes, but in later growth, they assume a hexagonal shape, extend in the lateral direction, and increase slightly in thickness. TEM images of the caps show stacking faults (Figure S2), ruling out screw-dislocation-driven growth. As

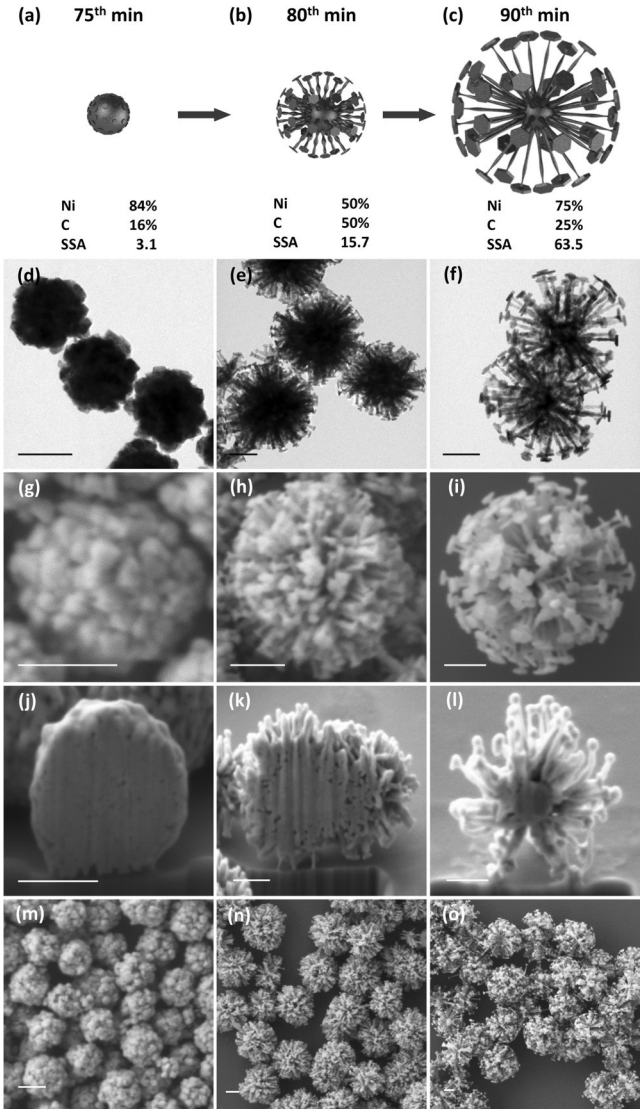

Figure 2. Time-resolved shape evolution of HNCs. The left, center, and right columns show the morphology of HNCs obtained after reactions of 75 (a) (d) (g) (j) (m), 80 (b) (e) (h) (k) (n), and 90 min (c) (f) (i) (l) (o), respectively. From the top of the Figure, each row corresponds to 3D illustrations (a)–(c), TEM BF images (d)–(f), SEM images (g)–(i), SEM images of FIB-milled cross-sections (j)–(l), and lower-magnification SEM images (m)–(o). Scale bars: 200 nm.

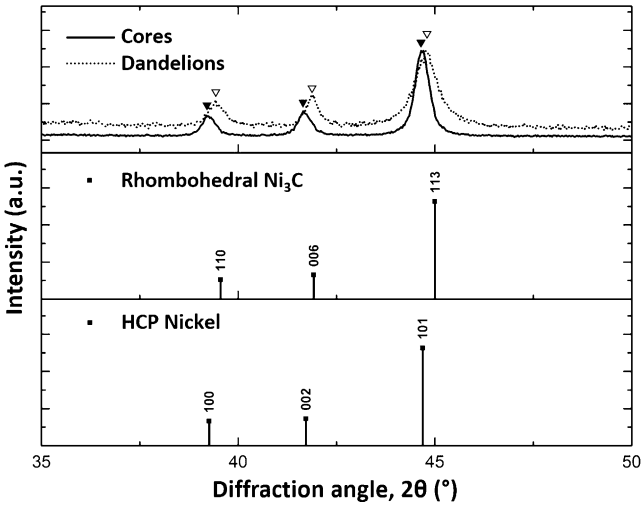

Figure 3. XRD patterns of the NCs and reference stick spectra for rhombohedral Ni_3C, and HCP Ni.

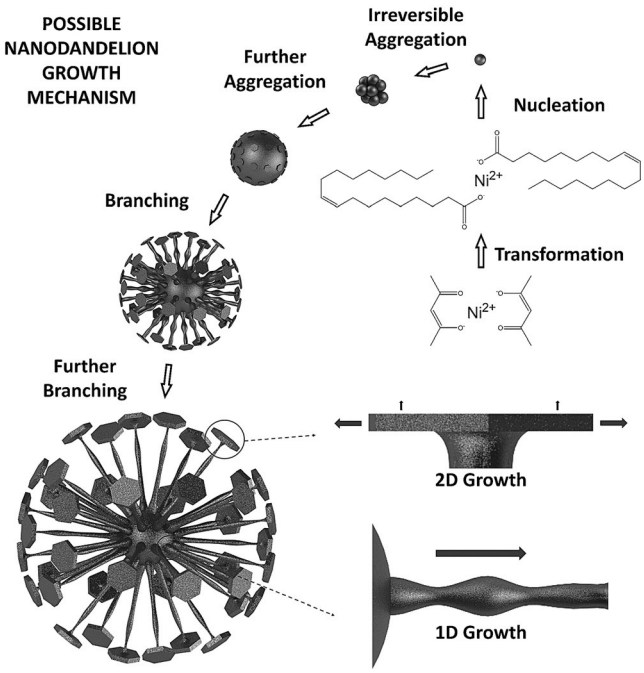

Figure 4. Proposed formation mechanism of the hierarchical Ni_3C "dandelion" HNCs; see text for details.

the reaction proceeds from the 80th to 90th min, the growth in the lateral dimensions becomes significant, comparing Figures 2e and 2f, implying that lower monomer concentration favors lateral growth, which is consistent with the wedding cake growth mechanism. In addition to branches originating from primary particles in the cores, during the growth of the HNCs, bifurcation of branches may occur when new primary particles attach to the growing branches (Figure S2).

With respect to composition evolution, Ni NCs prepared in organic solvents at sufficiently high temperature are inevitably carburized by the solvent and ligands, which in this case include 1-octadecene, oleic acid, oleylamine, and 1,2-tetradecanediol. Nickel itself can catalyze the decomposition of hydrocarbons adsorbed to its surface at the reaction temperatures used here. Diffusion of carbon into the Ni NCs forms Ni_3C.[7] The highly hierarchical surface of the HNCs is associated with large variation in surface chemical potential. Thus, formation of HNCs is kinetically controlled and occurs significantly away from equilibrium. This requires an environment in which the chemical potential of the monomer is relatively high, compared to that which would be in equilibrium with the corresponding bulk solid. Based on the close relationship between the growth mechanism and the crystal lattice of the material, we believe the mechanisms observed here may apply more broadly to other NCs with hexagonal crystal symmetry, and we are currently investigating the

generalization of this mechanism of forming HNCs as well as their applications in electrocatalysis.

In summary, we developed a facile formula for creating unique hierarchical Ni_3C "dandelion" nanostructures with a specific surface area much larger than that of dense particles of comparable size. The time evolution of these structures was studied to optimize their synthesis and develop an understanding of their formation mechanism. The Ni_3C HNCs have potential applications in water splitting and other catalytic processes. Insights into their growth mechanism can enlighten further research on the controlled synthesis of hierarchical nanostructures in solution.

Acknowledgements

This research was supported in part by the New York State Center of Excellence in Materials Informatics.

Keywords: crystal growth · crystallization · nanostructure · nickel carbide

How to cite: *Angew. Chem. Int. Ed.* **2016**, *55*, 8023–8026
Angew. Chem. **2016**, *128*, 8155–8158

[1] Y. Gogotsi, *Nat. Mater.* **2015**, *14*, 1079–1080.
[2] M. Nie, P. K. Shen, Z. Wei, *J. Power Sources* **2007**, *167*, 69–73.
[3] E. Yang, H. Ji, J. Kim, H. Kim, Y. Jung, *Phys. Chem. Chem. Phys.* **2015**, *17*, 5000–5005.
[4] N. A. Fadil, G. Saravanan, G. V. Ramesh, F. Matsumoto, H. Yoshikawa, S. Ueda, T. Tanabe, T. Hara, S. Ishihara, H. Murakami, K. Ariga, H. Abe, *Chem. Commun.* **2014**, *50*, 6451–6453.
[5] A. V. Syugaev, N. V. Lyalina, S. F. Lomayeva, A. N. Maratkanova, *J. Solid State Electrochem.* **2016**, *20*, 775–784.
[6] V. Stolojan, Y. Tison, G. Y. Chen, R. Silva, *Nano Lett.* **2006**, *6*, 1837–1841.
[7] D. L. Leslie-Pelecky, X. Q. Zhang, S. H. Kim, M. Bonder, R. D. Rieke, *Chem. Mater.* **1998**, *10*, 164–171.
[8] a) Y. Yu, M. Guo, M. Yuan, W. Liu, J. Hu, *Biosens. Bioelectron.* **2016**, *77*, 215–219; b) R. T. K. Baker, N. S. Dudash, C. R. F. Lund, J. J. Chludzinski, *Fuel* **1985**, *64*, 1151–1156.
[9] L. Qiao, M. T. Swihart, *Adv. Colloid Interface Sci.* **2016**, DOI:10.1016/j.cis.2016.01.005.
[10] E. Ye, M. D. Regulacio, S.-Y. Zhang, X. J. Loh, M.-Y. Han, *Chem. Soc. Rev.* **2015**, *44*, 6001–6017.
[11] Y. Goto, K. Taniguchi, T. Omata, S. Otsuka-Yao-Matsuo, N. Ohashi, S. Ueda, H. Yoshikawa, Y. Yamashita, H. Oohashi, K. Kobayashi, *Chem. Mater.* **2008**, *20*, 4156–4160.
[12] M. F. Sarac, W.-C. Wu, J. B. Tracy, *Chem. Mater.* **2014**, *26*, 3057–3064.
[13] Y. T. Jeon, J. Y. Moon, G. H. Lee, J. Park, Y. Chang, *J. Phys. Chem. B* **2006**, *110*, 1187–1191.
[14] S. Nagakura, *J. Phys. Soc. Jpn.* **1957**, *12*, 482–494.
[15] L. He, *J. Magn. Magn. Mater.* **2010**, *322*, 1991–1993.
[16] J. Park, K. An, Y. Hwang, J. G. Park, H. J. Noh, J. Y. Kim, J. H. Park, N. M. Hwang, T. Hyeon, *Nat. Mater.* **2004**, *3*, 891–895.
[17] V. K. LaMer, R. H. Dinegar, *J. Am. Chem. Soc.* **1950**, *72*, 4847–4854.
[18] J. Park, V. Privman, E. Matijevic, *J. Phys. Chem. B* **2001**, *105*, 11630–11635.
[19] X. Yin, J. Shi, X. Niu, H. Huang, X. Wang, *Nano Lett.* **2015**, *15*, 7766–7772.

Received: April 8, 2016
Published online: May 11, 2016

